ELSEVIER

Quaternary Science Reviews 24 (2005) 1345–1360

QSR

Internal and forced climate variability during the last millennium: a model-data comparison using ensemble simulations

Hugues Goosse[a,*], Hans Renssen[b], Axel Timmermann[c], Raymond S. Bradley[d]

[a]*Université Catholique de Louvain, Institut d'Astronomie et de Géophysique G. Lemaître, Chemin du Cyclotron 2, B-1348 Louvain-la-Neuve, Belgium*
[b]*Faculty of Earth and Life Sciences, Vrije Universiteit Amsterdam, De Boelelaan 1085, 1081 HV Amsterdam, The Netherlands*
[c]*IPRC, SOEST, University of Hawaii, Honolulu, HI 96822, USA*
[d]*Department of Geosciences, University of Massachusetts, 611 North Pleasant Street Amherst, MA 01003-9297, USA*

Received 27 January 2004; accepted 24 December 2004

Abstract

A three-dimensional climate model was used to perform 25 simulations over the last millennium, which are driven by the main natural and anthropogenic forcing. The results are compared to available reconstructions in order to evaluate the relative contribution of internal and forced variability during this period. At hemispheric and nearly hemispheric scale, the impact of the forcing is clear in all the simulations and knowing the forced response provides already a large amount of information about the behaviour of the climate system. Besides, at regional and local scales, the forcing has only a weak contribution to the simulated variability compared to internal variability. This result could be used to refine our conception of Medieval Warm Period and Little Ice Age (MWP and LIA). They were hemispheric-scale phenomena, since the temperature averaged over the Northern Hemisphere was, respectively generally higher/lower during those periods because of a stronger/weaker external forcing at that time. Nevertheless, at local-scale, the sign of the internal temperature variations determines to what extent the forced response will be actually visible or even masked by internal noise. Because of this role of internal variability, synchronous peak temperatures during the MWP or LIA between different locations are unlikely.

1. Introduction

Reconstructions of surface temperature averaged over the Northern Hemisphere display relatively warm conditions at the beginning of the 2nd millennium AD, albeit cooler than in the late 20th century (e.g., Jones et al. 1998; Mann et al., 1999; Crowley and Lowery, 2000; Briffa et al., 2001; Briffa and Osborn, 2002; Esper et al., 2002). The amplitude of the variations of this Medieval Warm Period (MWP) as well as the timing of the temperature maximum differs in these various reconstructions but they agree that warm conditions ended before 1300 AD (e.g.; Bradley, 2000; Crowley and Lowery 2000; Grove 2001). The relatively cool conditions were followed by a slow temperature recovery at the end of the 14th century, after which a gradual cooling set in, leading to particularly cold conditions during the 17th and the early 19th centuries, which are the coldest period of the Little-Ice Age (LIA). This long-term cooling trend was interrupted by relatively short, warm periods, as for instance in the middle of the 18th century. The cold period ended in the 19th century and was followed by a warming in the 20th century which leveled off during the 1940s. The latest, relatively fast, increase of Northern Hemispheric temperature since the 1950s can be mainly attributed to anthropogenic greenhouse warming (e.g., Hegerl and North, 1997; Crowley, 2000; Bertrand et al., 2002; Stott et al., 2000; Meehl et al., 2002).

Despite historical accounts and multi-proxy evidence, there is presently no accepted definition of the MWP and the LIA. Because of that, some people suggest avoiding the use of these terms. Although on

*Corresponding author. Tel.: +32 10 47 32 98; fax: +32 10 47 47 22.
E-mail address: hgs@astr.ucl.ac.be (H. Goosse).

0277-3791/$ - see front matter © 2005 Elsevier Ltd. All rights reserved.
doi:10.1016/j.quascirev.2004.12.009

hemispheric scales all temperature reconstructions exhibit a general cooling tendency from the beginning of the 2nd millennium AD until the 19th century, it is still unclear whether the MWP and LIA were truly global phenomena or whether current temperature reconstructions reflect more regional conditions. Analysing a large number of records, Hughes and Diaz (1994) argued that, in some areas of the world, the temperatures were relatively high during the MWP, in particular in summer. However, in other regions such as the Southeastern United States or Southern Europe along the Mediterrranean Sea, the climate during that time was not different from the periods that preceded or followed. Furthermore, the timing of the various warm episodes was not synchronous between different regions, as also noticed by Crowley and Lowery (2000) and Bradley et al. (2003). The cooling during the LIA appears more coherent over the mid-latitudes of the Northern Hemisphere. However, not all regional records show a consistent and synchronous cooling (e.g. Bradley and Jones, 1992, 1993; Jones et al., 1998, 2001; Bradley, 2000; Mann et al., 2000).

Climate model simulations could be used to study the characteristics of the MWP and LIA as well as to gain insight into the mechanisms that caused these climate variations. When driven by estimates of solar and volcanic forcing, physical and statistical models reproduce quite well the low frequency evolution of the northern hemisphere surface temperature as deduced from proxy records over the period AD 1000–1850 (e.g., Crowley, 2000; Bertrand et al., 2002; Bauer et al., 2003; Gerber et al., 2003). This suggests that external forcing plays a key role as pacemaker of low-frequency variations. In order to simulate the observed warming of the last century, it has been necessary to include also anthropogenic forcings (e.g., Crowley, 2000; Stott et al., 2000; Bertrand et al., 2002; Meehl et al., 2002).

Climate models used for an assessment of externally forced millennial-scale variability have very low resolution and the majority of them are two-dimensional (i.e. latitude and altitude/depth are varying). As a consequence, their results could not be used to gain information on a regional basis, not even at a continental-scale. Potentially, such information could be obtained from the comprehensive, three-dimensional general circulation models (GCMs) but, because of the high computer-time requirements, only a few transient simulations spanning the last 500 years have been published up to now (e.g., Cubasch et al., 1997; Rind et al., 1999; Waple et al., 2002; Gonzalez-Rouco et al., 2003; Widmann and Tett, 2003). GCM simulations were used to compare simulated response patterns to external forcing with low-frequency patterns deduced from observations. Three-dimensional general circulation models were also used to study the physical processes which amplify the climate response to strong external forcing, for instance during the minimum in solar irradiance of the late 17th century (Shindell et al., 2001). In addition, unforced GCM simulations were used in order to compare patterns of internal low-frequency variability with those obtained from reconstructions (Jones et al., 1998; Collins et al., 2002).

To overcome the computing time constraints of GCMs, it is possible to use low resolution three-dimensional models including a simplified, but reasonable, representation of the most important physical processes. Such an approach has been taken by van der Schrier et al. (2002) who analysed sea level variations during the last millennium. As in the majority of studies using GCMs on time-scale longer than 150 years, van der Schrier et al. (2002) performed only one simulation for each experimental design. This may be enough to look at large-scale, low-frequency variations, to make process studies or to look at the patterns associated with a particular forcing. However, such an approach is problematic in the sense that the observed trajectory of the climate system is just one realization within an ensemble of possible (partly externally forced) trajectories. The same holds for a single model simulation. In both cases internally generated internal variability could mask the forced signal.

As a consequence, in the present study, our goal is to estimate the contributions of forced and internal variability in the Northern Hemispheric climate evolution during the last millennium. To do so, an ensemble of 25 simulations is performed with a three-dimensional model of intermediate complexity. The model includes an improved version of the atmospheric model used by van der Schrier et al. (2002) coupled to a coarse-resolution ocean-sea-ice general circulation model. First, the results of the ensemble simulation are compared to observations to test the skill of the model. In a second step, the model results are used to help in the interpretation of the reconstructed temperature time series. We address the question as to whether the MWP and the LIA are robust features which were forced by solar and volcanic activity or whether they are representations of internal climate noise. To structure our analysis, we discuss the comparisons of simulated and observed temperature time-series on three different spatial scales (hemispheric, continental and regional) and separately consider the evolution of spatial patterns. We only use reconstructed temperature time-series with high temporal resolution because a reasonable number of these types of reconstruction are available now, for various regions of the world, and because the comparison with model variables is relatively straightforward. Our analysis will cover the period 1000–1980 AD as most proxy data are not available for the last 20 years.

Another interesting perspective on the issue of externally generated climate variability is that of predictability. Lorenz (1975) introduced two kinds of

climate predictability. Predictability of the first kind describes the loss of information during a forecast due to initial condition uncertainties. Predictability of the second kind on the other hand is associated with the influence of non-stationary boundary conditions on the system's evolution. Climate predictability of the first kind has been investigated by Griffies and Bryan (1997) and Grötzner et al. (1999) using coupled GCMs and ensemble simulations. Their analysis focused on the potential predictability on decadal and interdecadal timescales. The idea of these ensemble studies was to explore the possibility that simulated preferred interdecadal climate modes associated with variations of the strength of the thermohaline circulation (Delworth et al., 1993; Timmermann et al., 1998) are predictable up to a decade or so in advance, given well-defined oceanic initial conditions. For non-stationary boundary conditions (solar, orbital, volcanic forcing) this problem turns into a predictability problem of the first and second kind. The goal of our study is to explore this type of "mixed" predictability for the climate of the last millennium.

Our paper is organized as follows: In Section 2, a description of the model and of the experimental design of our simulations is given as well as a brief description of the techniques used and the limitations of the study. Section 3 analyses the results of the simulation. We first study the large-scale evolution of annual mean temperatures during the last millennium. Then, we discuss the regional climate changes driven by the external forcing and finally the evolution of large-scale patterns. Section 4 includes a discussion of the results and Section 5 summarizes our main findings and puts them into a broader perspective.

2. Methods

2.1. Model description

ECBILT–CLIO is a three-dimensional coupled atmosphere–ocean–sea ice model (Goosse et al., 2001; Renssen et al., 2002). The atmospheric component is ECBILT2 (Opsteegh et al. 1998; Selten et al. 1999), a T21, 3-level quasi-geostrophic model, with simple parameterizations for the diabatic heating due to radiative fluxes, the release of latent heat, and the exchange of sensible heat with the surface and a dynamically passive stratospheric layer is included. In particular, synoptic variability associated with weather patterns is explicitly computed. As an extension to the quasi-geostrophic equations, an estimate of the neglected terms in the vorticity and thermodynamic equations is incorporated as a temporally and spatially varying forcing. This forcing is computed from the diagnostically derived vertical motion field. With these ageostrophic terms, the simulation of the Hadley circulation is considerably improved, resulting in a drastic improvement of the strength and position of the jet stream and transient eddy activity. The model contains a full hydrological cycle that is closed over land by a bucket model for soil moisture. Each bucket is connected to a nearby ocean grid point to define the river runoff. Accumulation of snow over land occurs in case of precipitation when the land temperature is below zero. Cloud cover is prescribed following a seasonally and geographically distributed climatology (D2 monthly data set of the International Satellite Cloud Climatology Project, ISCCP, Rossow et al., 1996). As a consequence, any feedback associated with changes in the cloud cover is not taken into account, with some potential impact on the model climate sensitivity.

The CLIO model (Goosse and Fichefet, 1999; Goosse et al., 1999) comprises a primitive equation, free-surface ocean general circulation model coupled to a thermodynamic-dynamic sea ice model. The ocean component includes a detailed formulation of boundary layer mixing based on Mellor and Yamada's (1982) level-2.5 turbulence closure scheme (Goosse et al., 1999), a parameterization of density-driven downslope flows (Campin and Goosse, 1999) as well as isopycnal diffusion and the Gent and McWilliams parameterization to represent the effect of meso-scale eddies in the ocean (Gent and McWilliams, 1990). The sea ice model takes into account the heat capacity of the snow-ice system, the storage of latent heat in brine pockets trapped inside the ice, the effect of the sub-grid-scale snow and ice thickness distributions on sea ice thermodynamics, the formation of snow ice under excessive snow loading and the existence of leads within the ice cover. Ice dynamics are calculated by assuming that sea ice behaves as a two-dimensional viscous-plastic continuum (Fichefet and Morales Maqueda, 1997). The horizontal resolution of CLIO is 3° in latitude and longitude and there are 20 unevenly spaced vertical levels in the ocean.

ECBILT–CLIO is coupled to the VECODE model that simulates the dynamics of two main terrestrial plant-functional types, forest and grassland, and desert as a third dummy type (Brovkin et al., 2002). It should be noted that the computed vegetation changes only affect the land-surface albedo in ECBILT–CLIO, and have no influence on other processes, e.g., soil hydrology.

The coupled model includes realistic topography and bathymetry. The only flux correction in ECBILT–CLIO is an artificial reduction of the precipitation by 8.5% over the Atlantic and by 25% over the Arctic. The corresponding water is redistributed homogeneously over the North Pacific (Goosse et al., 2001). The model simulates relatively well the climate outside tropical regions (Goosse et al., 2001; Renssen et al., 2002). Its

sensitivity to a CO_2 doubling is 1.8 °C, which is in the low range of coupled atmosphere–sea-ice–ocean general circulation models. More information about the model and a complete list of references is available at the address http://www.knmi.nl/onderzk/CKO/ecbilt-papers.html.

2.2. Experimental design

Twenty-five simulations have been performed covering the last millennium. The evolution of solar irradiance follows the reconstruction of Lean et al. (1995) extended back in time by Bard et al. (2000). The variations of orbital parameters are taken into account (Berger, 1978). The effect of volcanism is derived from Crowley (2000) and is included through changes in solar irradiance. The influence of sulfate aerosols of anthropogenic origin is included through a modification of surface albedo (Charlson et al., 1991), the spatial and temporal distribution of the changes being derived from Boucher and Pham (2002). As a consequence, for the latter two forcings, we do not take into account the vertical distribution of the forcing or changes in longwave fluxes caused by the presence of the aerosols.

In addition, the observed evolution of well-mixed greenhouse gases (based on a compilation of ice cores measurements, J. Flueckiger, pers. comm., 2004) is imposed as well as the forcing associated with tropospheric ozone changes. The forcing due to change in land-use is based on Ramankutty and Foley (1999) and is applied in the model through a reduction of the area covered by trees and an increase in grassland as VECODE does not include a specific vegetation type corresponding to cropland.

The 25 simulations are all driven by the same forcing and differ only in their initial conditions. They were taken from previous experiments covering the last millennium (Goosse et al., 2004), each initial state selected being separated from the other ones by at least 150 years.

2.3. Type of analysis proposed

To analyse the variability, we consider different aspects of the simulated time-series. First, we analyse the individual ensemble members. In particular, the mean standard deviation of the ensemble members gives an indication of the total variability of the ensemble set that could be directly compared to the one deduced from observations (Table 1). Secondly, in order to reduce the level of internal climate variability and to keep a physical interpretation of the patterns, we compute the ensemble mean. This provides a measure of the thermodynamic response of the system to the forcing and of the robust changes of atmospheric or oceanic circulation driven by forcing variations. Its standard deviation gives thus an estimate of the magnitude of the forced response in the model (Table 1).

Third, it is useful to measure the spread of the various ensemble members around the mean caused by internal variability. This could be estimated directly, for each time period, as the standard deviation of the ensemble. The standard deviation is thus estimated from a sample of 25 elements and is potentially different each year. Nevertheless, as illustrated in Fig. 1, this standard deviation for surface temperatures is nearly constant in our experiment. For the hemispheric mean temperature, the values are a bit larger at the beginning of the experiments, because of the uncertainties in the initial conditions, but the differences are not significant. Nevertheless, this influence of the initial conditions could be much larger for other variables such as the ocean temperature at depth or the ice extent in the Southern Hemisphere, inducing a much higher standard deviation during the first centuries of the simulations (Goosse and Renssen, 2005).

An alternative way to estimate the internal variability of the modeled system is to compute the standard deviation of ensemble members after subtraction of the ensemble mean (i.e. thus removing the forced variations) (Table 1). Fortunately, those two measures of internal variability are perfectly compatible for surface temperature in our experiments. Indeed, thanks to the large sample used, the time average of the standard deviation of the ensemble is nearly identical to the standard deviation of ensemble members after subtraction of the ensemble mean, the difference between the two being generally smaller than 0.01 K.

2.4. Limitations

Before presenting the main results, it is good to realize that several sources of uncertainties are involved. Although the model used here is probably one of the more complex that could be used for ensemble simulations over the last millennium, it is not perfect, as any model. For instance, because of model resolution and the hypothesis applied, the tropical dynamics are not very well resolved, the topography is smoothed with a clear impact on the climate of some regions and the model does not include a representation of the stratospheric dynamics. In addition, large uncertainties exist on forcing variations during the last millennium with consequences on simulated temperatures (e.g., Lean et al., 1995; Crowley, 2000; Robertson et al., 2001; Bertrand et al., 2002; Bauer et al., 2003; Gerber et al., 2003).

Furthermore, proxy data do not provide a perfect record of past climate evolution. Various climatic and non-climatic variables could influence the record, making the extraction of the temperature signal and the calibration of proxies against instrumental data

Table 1
Standard deviation of the surface temperature in various reconstructions and in the model simulations

	Data			Mean σ of the ensemble ('Total variability')			σ ensemble mean ('Forced variability')			Mean σ series—ensemble mean ('Internal variability')		
	1-yr	10-yr	50-yr	1-yr	10-yr	50-yr	1-yr	10-yr	50-yr	1-yr	10-yr	50-yr
NH annual mean	0.13[1]	0.10	0.07	0.17	**0.11**	**0.10**	0.11	0.09	0.09	0.13	0.06	0.03
	—	0.10[2]	0.17									
NH summer (>20°N)	0.23[3]	0.16	0.12	**0.21**	0.12	**0.10**	0.12	0.10	0.10	0.16	0.07	0.03
	0.14[4]	0.12	0.09									
NH summer (>20°N) (1400–1960)	0.22[5]	0.15	0.13	**0.19**	**0.12**	**0.12**	0.15	0.08	0.11	0.16	0.06	0.03
30–70°N annual mean (1600–1980)	0.21[6]	0.19	0.17	**0.24**	**0.15**	**0.16**	0.14	0.13	0.16	0.19	0.08	0.05
Arctic				1.07	0.54	0.47	0.40	0.34	0.43	0.99	0.42	0.20
North America annual mean (1750–1980)	0.45[6]	0.33	0.27	0.81	**0.33**	**0.26**	0.26	0.19	0.23	0.77	0.28	0.12
Europe annual mean (1750–1980)	0.30[6]	0.14	0.09	0.54	0.23	0.17	0.18	0.13	0.15	0.51	0.20	0.09
Europe summer (1750–1980)	0.12[6]	0.09	0.06	0.51	0.20	0.12	0.18	0.10	0.08	0.58	0.18	0.09
Europe winter (1750–1980)	0.20[6]	0.10	0.07	1.02	0.41	0.27	0.28	0.20	0.22	0.98	0.35	0.16
Europe annual mean (1500–1980)	0.40[7]	0.18	0.17	0.54	**0.22**	**0.15**	0.16	0.11	0.12	0.51	0.20	0.09
Europe summer (1500–1980)	0.41[7]	0.23	0.17	0.61	**0.20**	0.11	0.18	0.09	0.07	0.58	0.18	0.08
Europe winter (1500–1980)	1.06[7]	0.36	0.33	**1.02**	**0.38**	0.23	0.26	0.17	0.18	0.98	0.34	0.15
Northern Europe (1620–1980)	0.65[5]	0.34	0.29	**0.64**	0.23	0.12	0.16	0.08	0.07	0.62	0.21	0.09
Southern Europe (1620–1980)	0.53[5]	0.36	0.35	**0.61**	0.20	0.11	0.17	0.09	0.07	0.60	0.17	0.08
Northern Siberia (1400–1980)	0.73[5]	0.58	0.50	0.92	0.30	0.17	0.22	0.11	0.10	0.89	0.29	0.12
Eastern Siberia (1400–1980)	0.42[5]	0.29	0.22	0.60	**0.26**	**0.16**	0.26	0.18	0.13	0.49	0.19	0.08
Patagonia summer	0.61[8]	0.21	0.11	1.28	0.42	0.20	0.27	0.11	0.08	1.25	0.41	0.18
Fennoscandia summer	0.64[9]	0.36	0.29	0.92	**0.40**	**0.21**	0.22	0.14	0.14	0.89	0.37	0.15

Unless specified, the statistics are computed over the period 1000–1980 AD. For each time series, the standard deviation is computed from the original time series including interannual changes (column 1 yr), for the time series grouped in 10-year averages (column 10 yr) and in 50-year averages (column 50 yr). For the model experiments, the standard deviation averaged over the 25 members of the ensemble is presented first. This could be compared directly with the standard deviation of the reconstructions. The standard deviation of the ensemble mean is also displayed as well as the mean standard deviation of the 25 simulations from which the ensemble mean has been subtracted. The data sources are:[1]Mann et al. (1999), [2]Crowley and Lowery (2000), [3]Jones et al. (1999), [4]Briffa (2000), [5]Briffa et al. (2001), [6]Mann et al. (2000), [7]Luterbacher et al. (2003), [8]Briffa et al. (1992) and [9]Villalba (1990). When the model standard deviation is in agreement with the standard deviation of the data at the 95% level, the corresponding number is in bold. This confidence level as been computed assuming that the variance ratios are *F*-distributed and taking into account the autocorrelation of the times series as proposed in Wilks (1995).

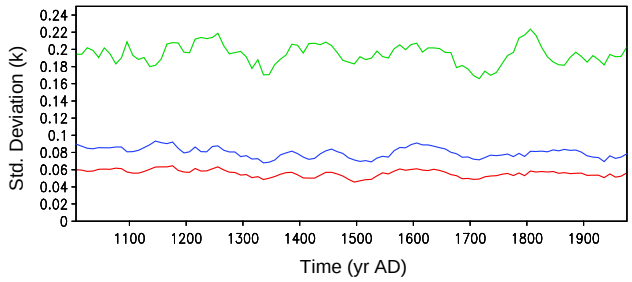

Fig. 1. Time series of the standard deviation of the ensemble for the annual mean temperature in the northern hemisphere (red), the annual mean temperature between 30° and 70°N (blue) and the annual mean temperature over Europe (green).

difficult. For instance, there are large uncertainties in the seasonal dependency of proxies such as tree rings. Furthermore, it is well documented that different proxies exhibit a different spectral sensitivity to climatic variations. Proxies can also be influenced by the local climate, while models give estimates of variations on scales of hundred of kilometers. These problems are presently under investigation and shall not be discussed here. We will make the optimistic hypothesis that proxies provide an unbiased and precise estimate of past climate variations. At least, we will consider that the proxies are precise enough not to alter the validity of our conclusion. This will be tested by using different data sets. Despite these caveats and uncertainties, our results provide a first step towards a systematical comparison of model results and reconstructions of the recent evolution of the climate system.

3. Results

3.1. Large-scale evolution of the surface temperature

Fig. 2 shows the time series of solar and volcanic forcing, the simulated temperatures and the reconstructed temperature data from Mann et al. (1999), Crowley and Lowery (2000), Jones et al. (1998), Briffa et al. (2001) and Briffa (2000). In the Northern Hemisphere, the phase of the ensemble mean follows closely the evolution of the external forcing. However, the amplitude of the temperature variations depends strongly on the season and the area over which the average is performed. Overall, the reconstructed temperatures covary with the simulated ensemble both in phase and amplitude. One noticeable discrepancy between the reconstructed temperatures and the ensemble occurs at the end of the 19th century when the model overestimates the temperature, at least on annual mean. As argued in some recent studies, the climate during this period appears strongly influenced by changes in land-use (e.g., Bertrand et al., 2002; Bauer et al., 2003). The discrepancy between model results and the reconstructions might thus be due to an underestimation of the response to this forcing in our simulations.

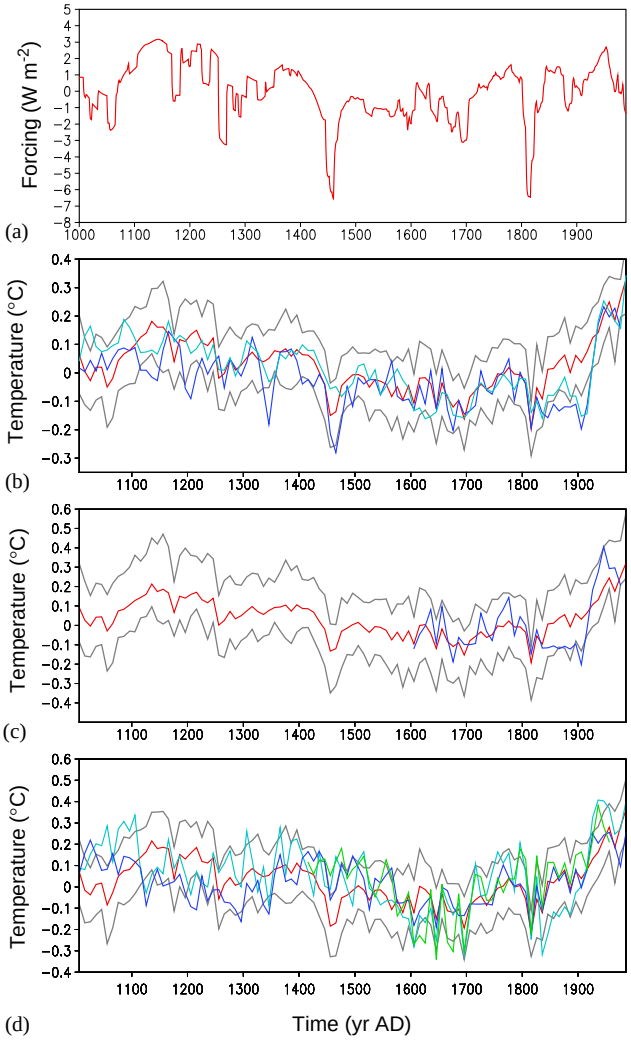

Fig. 2. (a) Effective solar forcing at the top of the atmosphere associated with variations in solar irradiance and volcanic eruptions. A 15-year running mean has been applied to the time series. (b) Anomaly of annual mean surface temperature over the Northern Hemisphere averaged over 25 simulations that differ only in their initial conditions (red). The mean over the ensemble plus and minus two standard deviations of the ensemble are in grey. The temperature reconstructions are in dark and light blue (Mann et al., 1999; Crowley and Lowery, 2000). The reference period used for the computation of anomalies here and in the following figures is the period 1000–1750 AD, corresponding to pre-industrial conditions. (c) Same as figure (b) for the annual mean temperature between 30 and 70 °N. The reconstruction is in blue (Mann et al., 2000). (d) Same as figure (b) for the summer temperature (AMJJAS) on continents northwards of 20°N. The reconstructions are in light blue, dark blue and green (Jones et al., 1999; Briffa et al., 2001; Briffa et al., 2000). For (b–d), the time series have been grouped in 10-year averages before the computation of the standard deviation.

Table 1 shows that for interannual variations, the standard deviation of the ensemble mean (column 3) is

of the same order of magnitude as the mean standard deviation of the time series minus the ensemble mean (column 4). This shows that, for interannual variations, a large fraction is due to internal variability, as expected. When performing averages over 10 or 50-year periods, the standard deviation of the ensemble mean becomes clearly higher than the one associated with internal variability. At these long time scales, the forced response is thus responsible for a large fraction of the simulated variability. This conclusion is in agreement with the fact that models lacking any representation of internal variability were able to reproduce the past evolution of the temperatures at hemispheric scale when driven by the appropriate forcing (Crowley, 2000; Bertrand et al., 2002; Bauer et al., 2003; Gerber et al., 2003).

The standard deviations for each ensemble member agree reasonably well with the observations. As can be seen from Fig. 2d, even the simulated low-frequency variations compare well with the reconstructions of Briffa et al. (2001) who used a technique devoted to preserve those low-frequency changes. Furthermore, the analysis of the results of Table 1 illustrates that there is no systematic bias of the model results at large scale in the Northern Hemisphere with respect to the observations.

3.2. Local and regional changes

3.2.1. Continental scale

At the scale of a large region such as the Arctic or at continental scale, the forced response follows the forcing (Fig. 3), as was already noticed for (nearly-) hemispheric averages in the Northern Hemisphere in Section 3.1. A clear and strong polar amplification is simulated in the model, with the amplitude of the variations being about 5 times stronger between 70° and 90°N than the hemispheric mean. This amplification is noticed all year long in the model but is particularly strong in winter. A polar amplification was noticed in a lot of model experiments, in particular those simulating future climate change, but it may be overestimated with respect to the tropical regions here as our model underestimates tropical variability. Nevertheless, Mann et al. (2000) also found, when comparing the temperature evolution during the last 4 centuries in various latitude bands, larger changes in mid and high latitudes (their analysis goes up to 70°N) than in the tropics. Unfortunately, the data of Overpeck et al. (1997) could not provide a direct measure of the amplification in Polar Regions as they only offer a relative evolution of the temperature. For Fig. 3a, this evolution has been scaled using the standard deviation of the model. This seems reasonable as the model simulates quite well the temperature evolution observed by means of thermometers during the last 120 years in Arctic regions (Goosse and Renssen, 2003).

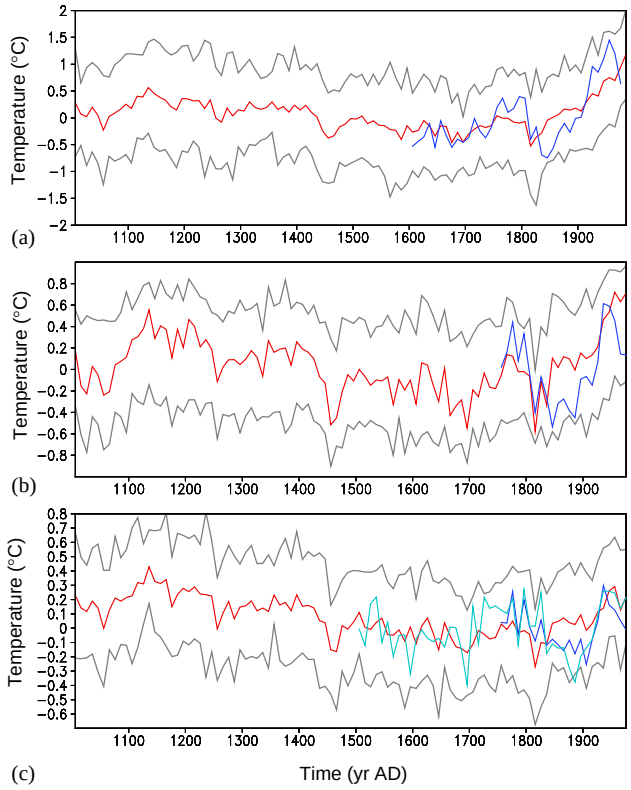

Fig. 3. Regional temperature evolution between 1000 and 1980 AD. (a) Anomaly of annual mean surface temperature between 70° and 90°N averaged over 25 simulations that differ only in their initial conditions (red). The mean over the ensemble plus and minus two standard deviation of the ensemble are in grey. The temperature reconstruction is in blue (Overpeck et al., 1997). (b) Same as figure (a) for the annual mean temperature in North America. The reconstruction is in blue (Mann et al., 2000). (c) Same as figure (b) for the annual mean temperature over Europe. The reconstructions are in dark blue (Mann et al., 2000) and light blue (Luterbacher et al., 2004). The time series have been grouped in 10-year averages.

As expected, the scatter between the various elements of the ensemble is much larger for temperature variations at continental scale than at hemispheric scale. For interannual changes, the standard deviation of the ensemble members after the ensemble mean is subtracted (internal variability) is more than 2 times larger than the standard deviation of the ensemble mean (forced variability, i.e. compare columns 3 and 4 in Table 1). In the Arctic, the standard deviation of the ensemble mean is large, but internal variability is large too, deteriorating the signal-to-noise separation. When performing averages over 10 or 50 years, the fraction of variability explained by variations of the forcing increases, but the contribution of internal variability is still responsible for a large fraction of the variations.

The annual mean model results also show some agreement with the reconstructions of Mann et al. (2000) and Luterbacher et al. (2004), when analysing both the time series (Fig. 3c) and the standard deviations

(Table 1). As in Mann et al. (2000), the simulated standard deviation is higher in North America than in Europe. Nevertheless, the model tends to significantly over estimate the variations in Europe compare to Mann et al. (2000), while the model standard deviation is closer to the reconstruction of Luterbacher et al. (2004).

Fig. 4a confirms that, in the model, the time evolution of the ensemble mean temperatures averaged over Europe and North America are quite similar and appears to be directly related to the forcing. We noticed a relative cooling trend in Europe compared to North America that is related to the deforestation in Europe during the last millennium. This indicates that, in our model simulations, the response to the forcing does not involve complex changes of the atmospheric and/or oceanic circulation that could lead, for instance, to different phasing of cold and warm periods in the two continents. The response seems to be generated mainly by local forcing, rather than by remote temperature changes which excite changes of the atmospheric and/or oceanic circulation.

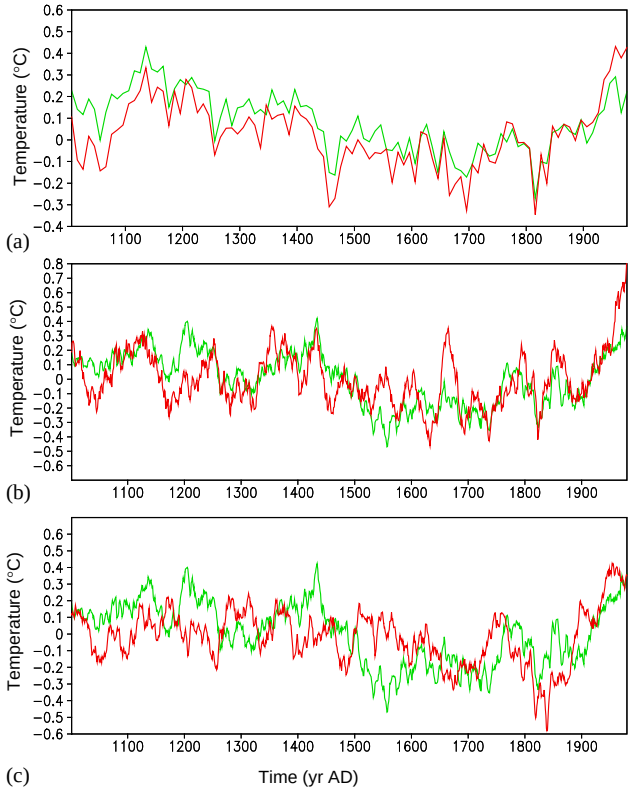

Fig. 4. Simulated temperature in Europe and North America. (a) Anomaly of annual mean surface temperature in Europe (green) and in Northern America (red) averaged over 25 simulations that differ only in their initial conditions. (b) Anomaly of annual mean surface temperature in Europe (green) and in Northern America (red) in one of the 25 simulations. (c) Anomaly of annual mean surface temperature in Europe in two of the 25 simulations.

Besides, when looking directly at the time series in one particular experiment, the differences between the two continents appear much larger than for the ensemble mean (Fig. 4b). The long-term tendencies are the same, but maximum cooling and warming occur at different times. For instance, in this simulation, the period around 1200 AD century appears quite cold in North America while Europe has relatively mild conditions. The real climate evolution corresponds to a particular realization of the response of the climate system to the forcing, as it is the case for one model simulation. If the model results are valid, this suggest that the difference between observed time series of temperature averaged over those two continents can be large during the last millennium, but they appear mainly due to internal variability, not to a different response to the forcing.

The comparison of the time evolution of the temperature in Europe in two individual simulations (Fig. 4c) shows that peak warming/cooling at continental scale occurs mainly by chance. The probability to have particularly warm/cold conditions is higher when the forcing imposes a warming/cooling but the exact timing is strongly influenced by the internal variability of the system. As a consequence, a maximum or minimum temperature occurs rarely twice at the same time in two different simulations. The peak cooling imposed by large volcanic eruptions is an exception (e.g., around 1810 AD), which is in agreement with Briffa et al. (1998). The magnitude of the cooling resulting from those events differs between the simulations but their effect is generally apparent in the majority of the simulations at continental scale.

It is also interesting to note that the temperature evolution in the two regions in the same experiment (Fig. 4b) looks more similar than the temperature evolution in the same region for two different experiments (Fig. 4c). This suggests that internal variability implies a kind of consistency between the different regions in a particular experiment. This is in agreement with the results of Jones et al. (1999) and Collins et al. (2002) showing that the dominant mode of variability in observations and in a model simulation without any external forcing has the same sign over a large part of the Northern Hemisphere.

As in Mann et al. (2000) and Luterbacher et al. (2004), the standard deviation of winter mean temperature in Europe is larger than in summer (Fig. 5). As we already noticed for the annual mean data, the model largely overestimates variability on all time-scales compared to the Mann et al. (2000) data set but is relatively close to Luterbacher et al. (2004). The forced response again looks quite similar in the two seasons with warm summers occurring during the same periods as warm winters. As a consequence, major differences between the summer and winter temperature evolution recorded in data (e.g., Shabalova and Van Engelen,

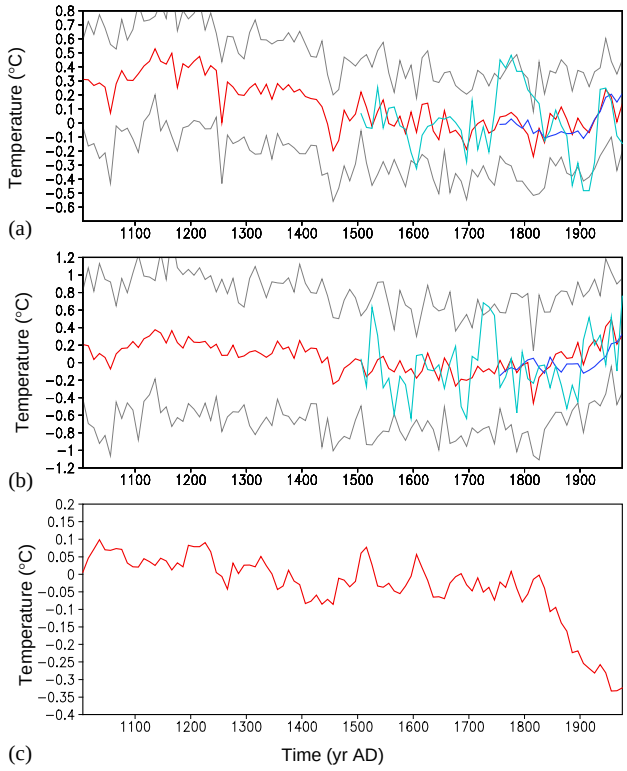

Fig. 5. Seasonal variations of temperatures in Europe. (a) Anomaly of summer mean temperature in Europe averaged over 25 simulations that differ only in their initial conditions. The mean over the ensemble plus and minus two standard deviations of the ensemble are in grey. The reconstructions are in dark blue (Mann et al., 2000) and light blue (Luterbacher et al., 2004). (b) Same as figure (a) for the winter mean temperature in Europe. The reconstructions are in dark blue (Mann et al., 2000) and light blue (Luterbacher et al., 2004). (c) Seasonal range (summer minus winter temperatures) over Europe averaged over 25 simulations that differs only in their initial conditions. The time series have been grouped in 10-year averages.

2003) should be, according to our results, mainly related to internal variability for the time and spatial scales investigated here.

Nevertheless, a closer look at the temporal changes in the seasonal contrast between summer and winter indicate a decrease at a relatively constant rate of about 0.01 K per century over the period 1000–1850 AD and at a large rate of about 0.2 K per century over the last 150 years (Fig. 5c). This results in a total decrease of the difference between summer and winter temperatures in Europe of nearly 0.5 K over the past millennium and thus a clear warming in winter relative to summer during this period. This reduction of the seasonal contrast is in agreement with observations (e.g., Thomson, 1995; Jones et al., 2003). In particular, Jones et al. (2003) discuss the potential impact of this result on the calibration of proxy records.

The long term decrease in seasonal contrast is mainly due orbital forcing which implies a decrease of $0.33\,W\,m^{-2}$ in summer insolation and an increase of $0.83\,W\,m^{-2}$ in winter at 45°N during the past millennium. This hypothesis is confirmed by the analysis of a previous set of experiments (Goosse et al., 2004) covering the last millennium but that does not include orbital changes. Indeed, in those experiments, no long-term trend is obtained in the seasonal temperature contrast in Europe for the period 1000–1800 AD. Besides, the large winter warming in Europe during the last century is due to a stronger response in winter than in summer to greenhouse gas forcing (for more information about the seasonal dependence of the response to this forcing, see for instance Manabe et al., 1992).

3.2.2. Sub-continental and regional scales

Because of its coarse resolution, our model is not well adapted to study the climate evolution at regional scales in detail. Nevertheless it is interesting to check if the general conclusions obtained for continental scales are valid on smaller scales. This appears to be the case as for regional scales the forced response generally follows the forcing, but it is responsible for an even smaller fraction of the variations than at continental scale (Fig. 6). Indeed, when performing a 50-year average, the internal variability still represents the major contribution. The relative contribution of internal variability appears particularly large in some regions like in Patagonia (Table 1), thereby making a signal-to-noise separation very difficult. As a consequence, the maximum temperatures at those scales can be found at periods separated by more than 100 years in two different simulations. Any attempt to define optimal conditions such as the medieval warm period based on such time series would thus be strongly biased towards internal variability in this region since individual sub-continental time series do not necessarily reflect global or forced variations.

The model results agree reasonably well with some observations even on regional scales (like for Fennoscandia, Fig. 6c), but in general the model underestimates the variations in Europe (Fig. 6a and b) compared to the reconstruction of Briffa et al. (2001). As already mentioned, the goal of Briffa et al. (2001) was to preserve low frequency variations in their reconstruction. This leads to standard deviations that are higher than those of other data sets but also higher than in the model at low frequency.

3.3. Large-scale spatial patterns

In previous sub-sections, we have analysed the time evolution of the temperature in different regions. However, complementary information can be obtained from the spatial distribution of the changes as proposed in this section. To do so, we compute 25-year averages

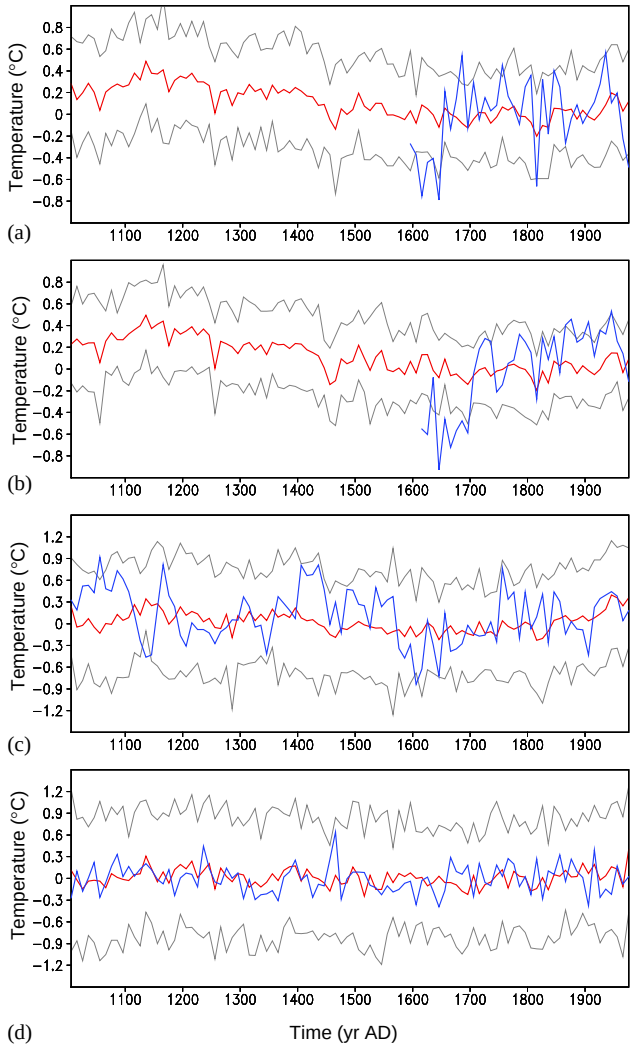

Fig. 6. Local temperature: (a) Anomaly of summer mean temperature in Northern Europe averaged over 25 simulations that differ only in their initial conditions. The mean over the ensemble plus and minus two standard deviations of the ensemble are in grey. The reconstruction is in blue (Briffa et al., 2001). (b) Same as figure (a) for the Southern Europe. (c) same as (a) for Fennoscandia. The reconstruction is in blue (Briffa et al., 1992). (d) Same as (a) for summer temperature over Patagonia. The reconstruction is in blue (Villalba, 1990). The time series have been grouped in 10-year averages.

over a particularly warm period in the Northern Hemisphere (see Fig. 2b), but similar conclusions could be drawn for other warm or cold periods. The mean of the 25 simulations displays quite a homogenous monopole-like response for nearly all the model grid points in the hemisphere (Fig. 7a). Nevertheless, the magnitude of the response differs strongly for various regions. This is firstly related to the polar amplification already noticed for large-scale averages (Fig. 3). Secondly, the temperature changes are much larger over the continents than over the open oceans, which is understandable in terms of local forcing operating on two different systems with different heat capacity.

In a particular experiment (Fig. 7b), the temperatures also tend to have the same sign as displayed for the ensemble mean (Fig. 7a). This is clearly related to the low scatter of (nearly-) hemispheric mean for the various simulations and the importance of the forcing at this scale. Nevertheless, for numerous areas, the temperature changes are weak, making the period under consideration not exceptional. In some areas, even the sign is opposite to the hemispheric mean. This is consistent with preliminary results which were based on two simulations performed over the last 500 years using two different general circulation models (Widmann and Tett, 2003). As a consequence, even for the 25-year-long averages (which includes an important contribution of the large-scale response to the forcing), it is impossible to guarantee that the sign of the temperature change at a particular location could be predicted even when the hemispheric mean is known. Indeed, the internal and regional variability could easily overwhelm the tendency imposed by the forcing at those scales.

This behaviour could be evaluated in a more formal way by computing the forced fractional variance (Fig. 8), as estimated by dividing the variance of the ensemble mean by the mean variance of the individual members (this is similar to dividing the square of the values of the column 3 of Table 1 by the square of the values of the column 2). For 10-year averages, at the model grid-scale, the value of this ratio is generally lower than 0.3. On the other hand, values are generally higher than 0.4 for 50 year averages, confirming that, for low-frequency changes, the forced response provides a larger contribution than at high frequencies. Nevertheless, even for 50-year averages, the role internal variability could by no means be neglected, as underlined above. In particular, internal variability is still clearly dominant in some regions like the Greenland Sea and the Central North America.

It is not our purpose here to look into details of changes in atmospheric or oceanic conditions related to forcing variations. Nevertheless, because of the large current interest in this subject, we cannot avoid describing the simulated changes in the North Atlantic Oscillation indices or of the closely related Arctic Oscillation (also known as the Northern Annular Mode). The first principal component (or first Empirical Orthogonal Function) of the geopotential at 850 hp in the model is an annular mode similar to the AO (Goosse et al., 2001). The time series of this mode, averaged over the 25 simulation displays very small variations, showing that the contribution of the forcing to low-frequency changes in this mode is nearly negligible in the model (Fig. 9a). This result manifests itself in that the variations of the atmospheric circulation are mostly driven by internal dynamics, rather than by external long-term forcing changes. The 20th century is an exception with a significant forced response. As a

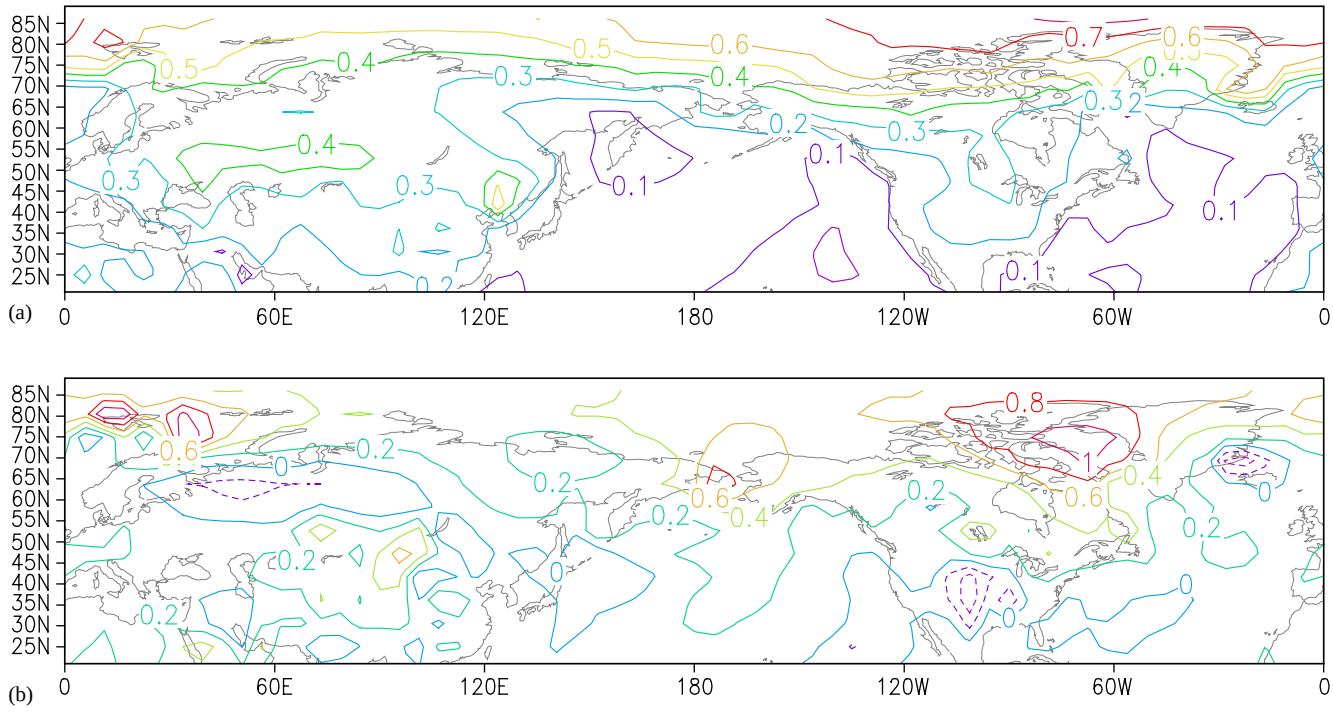

Fig. 7. Simulated annual mean surface temperature for a particularly warm period on Northern Hemisphere mean (1125–1150 AD). (a) Averaged over 25 simulations that differ only in their initial conditions and (b) in one typical member of the ensemble.

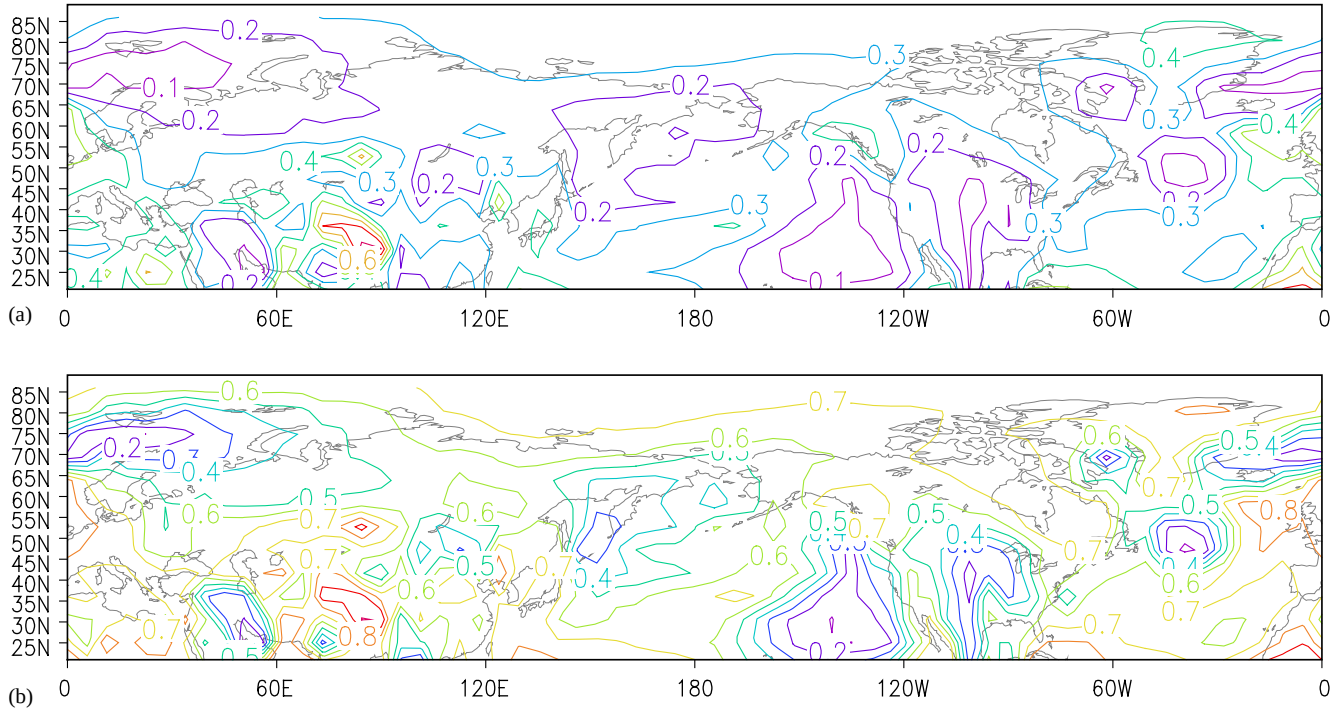

Fig. 8. Variance of the ensemble mean divided by the mean variance of the individual members (a measure of the forced response at local scale) for (a) 10-year averages and (b) 50-year averages.

consequence, a combination of this positive trend at the end of the experiments with an increase due to internal variability could lead to a large increase in the index during this period. Nevertheless, the forced response is not large enough to completely overwhelm the internal variability and the late 20th century in the majority of

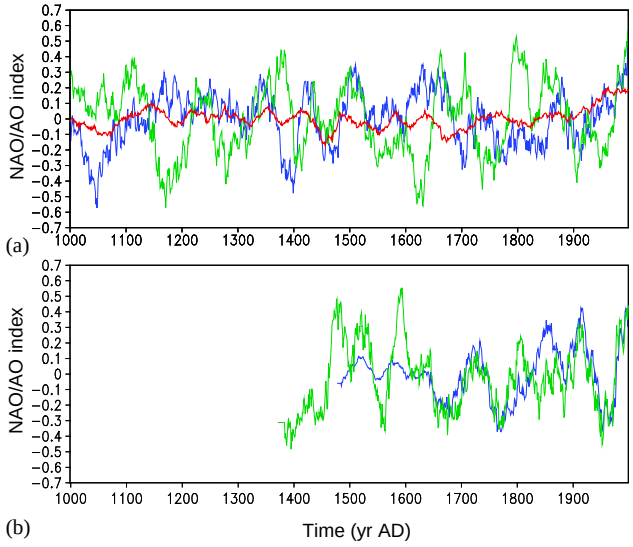

Fig. 9. NAO-AO index: (a) Time series of the first principal components of geopotential height at 850 hp for the area northward of 20°N, averaged over the 25 simulations (red) and for two typical members of the ensemble (green and blue) (b) NAO index reconstructions of Cook et al. (2002) in blue and Luterbacher et al. (2002) in green. The Cook et al. (2002) reconstruction has been scaled on the figure to have the same variance as the one of Luterbacher et al. (2002).

the simulations does not appear as clearly anomalous compared to earlier periods in the model (e.g., Fig. 9a). This result is consistent with available long-term reconstructions (Fig. 9b).

The individual members display low frequency variations, with prolonged periods where the time series tend to be positive (or negative), as in reconstructions of the NAO index (Fig. 9). Nevertheless, those periods are associated with the internal variability of the model, and they occur at different times in the various simulations.

In a recent study of the quasi-equilibrium response to changes in solar irradiance, Shindell et al. (2001) show that a change in solar input is associated with a shift in the AO/NAO index in their model, because of modifications in the stratosphere. In ECBILT–CLIO, changes in solar irradiance have also an impact on the atmospheric circulation (Goosse and Renssen, 2004) but this is related to different processes as the model does not include an interactive representation of stratospheric dynamics. Indeed, in our model, a warming at high latitude driven by the external forcing induces a decrease of geopotential height at 850 hp (or surface pressure) that is associated with stronger zonal winds at mid-latitude and thus characteristics similar to the ones associated with a positive NAO/AO index (for more details, see Goosse and Renssen, 2004). Nevertheless, the magnitude of the changes are smaller in our model than in Shindell et al. (2001), probably because our model does not include stratospheric dynamics. Fig. 9 shows that, in our simulations, this forced response is too weak to play a key role using the forcing applied, at least during the pre-industrial period. Note that discrepancies are also found between different models when analysing the impact of the recent and future increase in greenhouse gas concentration on the evolution of the NAO/AO index and in particular on the exact role of stratospheric dynamics (e.g., Shindell et al., 1999; Zorita and González-Rouco, 2000; Gillett et al., 2002, 2003; Paeth et al., 2003).

4. Discussion

We have presented here results of an ensemble of 25 simulations performed with a coupled atmosphere–ocean–sea-ice model in order to highlight the relative contribution of internal and forced variability during the last millennium. This is a very broad subject, and this first study can be considered as an introduction. First of all, we have presented time series for particular areas to highlight some important processes, but our conclusions could certainly not be naively translated to any part of the world. Some further detailed studies of the regional characteristics of the simulated climate evolution during the last millennium are thus needed. Secondly, our conclusions are based on the results of a single model. Although they are consistent with available data, using other more comprehensive coupled general circulation models will help to refine our findings or even to determine where we were probably wrong.

Despite the limitations of our study, the various times series of reconstructed climate show that the proxy data are generally within the range of the simulated model variability. This is a necessary first step, but if the model variability is large enough, any observation could fit in model range. The model variability has thus to be compared to the variability of the reconstructions. In our experiments, the simulated standard deviation of the temperature at various scales is in reasonably good agreement with observations. The model is also able to reproduce qualitatively the differences between the regions or the seasons deduced from observations. Nevertheless, the simulated variability is too weak compared to the reconstruction of Briffa et al. (2001) that exhibits a larger standard deviation than in other data sets, particularly on regional scales.

If we consider that this higher level of variability is reasonable, four elements could explain why the model underestimates this level. Firstly, there are large uncertainties in the forcing time series, in particular for low frequency. An underestimation of these forcing variations could thus have an impact on the response simulated by the model. Secondly, the sensitivity of our model, which is in the lower range of estimates made for climate models, could be too weak. Thirdly, the model could underestimate the internal climate variability of the system at regional scales. This would be in

agreement with the results of Stott and Tett (1998) who found that their coupled GCM underestimates observed unforced variability at spatial scales less than 2000 km. A fourth hypothesis is that internal modes of variability are not amplified sufficiently by the forcing. Unfortunately, it is presently not possible to determine which of these hypotheses play an important role because of the lack of sufficiently precise information on all those processes.

Our analyses have not been focussed on the recent warming but we can make a few remarks here. The increase of the forcing during the 20th century is larger than during other periods. In the model simulations, there is not a significant increase of the scatter between the different members of the ensemble of simulation during this period. As a consequence, the relative contribution of the forcing on temperature variations on regional scales is larger than for earlier periods, thereby facilitating a signal-to-noise separation. Still, there are many locations that do not display an unusual 20th century warming. However, as the forcing is expected to increase in future, we expect that the number of locations where this warming trend is not yet visible will strongly diminish. According to Stott and Tett (1998), the detection of such a warming at all spatial scales will become highly probable by the middle of the 21st century.

5. Conclusions

The ensemble simulations performed here have been documented to be very useful in a thorough model-data comparison. They have also been used to underline some basic characteristics of the forced climate system. First of all, the relative contribution of forced and internal variability in the model during the last millennium has been described. The mean of the 25 simulations appears more or less directly driven by the forcing in our model on regional and hemispheric scales. For (nearly-) hemispheric averages, the scatter around this ensemble mean is small. As a consequence, the impact of the forcing is clear in all the simulations. Knowing this forced response provides already a large amount of information about the behaviour of the climate system on these scales.

For regional or local scales, the forced response explains a smaller fraction of the simulated variability. At a local scale, the forcing has only a weak contribution in the simulated variability and the signal-to-noise separation becomes much more difficult. The relative contribution of forced and internal variability is also dependent on the time scale. For interannual changes, even the large-scale response is strongly influenced by internal variability, while decadal variations phase-lock with the forcing much more easily.

The exact contribution of forced and internal variability is certainly model dependent. Nevertheless, the large role of the forcing for low frequency, large scale variations as well as the importance of internal modes of variability for high frequency and regional changes appear robust and well in agreement with previous model studies. This conclusion could be used to refine our concepts of the Medieval Warm Period and Little Ice Age.

Our results suggest that the MWP was a hemispheric-scale phenomenon, at least, since the temperature averaged over the Northern Hemisphere was generally higher during the period 1000–1200 AD than during the following centuries. According to presently available forcing time series, this is the consequence of a global forcing, external to the climate system itself. The large-scale low-frequency average filters the internal variability and allows detection of this weak forcing.

On local and regional scales, this external forcing results also in a higher probability for any location to have warm conditions than cold ones during the MWP. Nevertheless, the sign of the internal temperature variations determines whether the forced response will be actually visible or even overcompensated by internal noise. Because of this role of internal variability, synchronous peak temperatures during the MWP between different locations are unlikely to have occurred. Furthermore, saying that warm conditions at one location are the local-manifestation of MWP could be misleading. It is reasonable to consider that such warm local conditions are mainly linked to local or regional processes. If such favourable processes enhance the small background temperature increase due to the forcing, it could be part of the MWP, but it could also occur later when the forcing is low, and has thus no relationship with the large-scale phenomena. The same conclusions hold for the LIA. Nevertheless, for cold periods, the forcing could be stronger mainly because of the huge effect of some volcanoes and the cooling could be more easily seen on some local time series.

In our simulations, the forcing imposes a response of the same sign nearly everywhere, with an amplification of the changes over the continent and at high latitudes. Large-scale changes in ocean and atmospheric circulation do not appear to have a dominant role in the forced temperature evolution. In particular, the changes of the North Atlantic Oscillation/Arctic Oscillation imposed by the forcing are quite weak in the model, except during the 20th century, which is not contradicted by available reconstructions. In each of the simulations, NAO/AO has of course an impact on the regional temperature evolution, but it is related to the internal variability in the model.

This model result has to be taken with great caution as a lot of uncertainties still exist on the impact of external forcing on the NAO/AO. Furthermore, we are

only able to test the response of the physical processes well represented in the model and processes not included might imply a different behaviour. In order to gain further insight in the relative contribution of internal and forced variability processes, additional transient multi-century ensembles would be very helpful to compare results of various models with high-quality data during periods where a forced response is supposed to have occurred in the past.

The weak response of the NAO/AO index in the model does not at all mean that there is no change in the atmospheric and or oceanic circulation in the model or that such changes have only a weak impact on the temperature. More studies are needed however to assess the impact of external forcing on the atmospheric circulation more quantitatively for the different regions. Furthermore, we present only seasonal averages, not focussed on any particular processes. For instance, using the same kind of simulation but more specific diagnostics, Goosse and Renssen (2004) have shown that the probability of having a particularly cold year in the Nordic Seas, which is related to changes in oceanic and atmospheric heat transport towards this area, is clearly dependent on the forcing.

Acknowledgements

The majority of the data sets used in this study were obtained from the World data Center for climatology hosted by NOAA (http://www.ngdc.noaa.gov/paleo/data.html). H. Goosse is Research Associate with the Fonds National de la Recherche Scientifique (Belgium). This study was carried out as part of the Second Multiannual Scientific Support Plan for a Sustainable Development Policy (Belgian Federal Science Policy Office, contracts EV/10/7D and EV/10/9A). A. Timmermann has been supported by the Collaborative Research Effort SFB 460 of the Deutsche Forschungs Gemeinschaft and by the Japan Agency for Marine-Earth Science and Technology (JAMSTEC) through its sponsorship of the International Pacific Research Center. H. Renssen is sponsored by the Netherlands Organization for Scientific Research (NWO). All these supports are gratefully acknowledged. We would also like to thank J. Luterbacher for sending us his temperature data for Europe. This is IPRC publication number 309 and SOEST publication number 6541.

References

Bard, E., Raisbeck, G., Yiou, F., Jouzel, J., 2000. Solar irradiance during the last 1200 years based on cosmogenic nuclides. Tellus 52B, 985–992.

Bauer, E., Claussen, M., Brovkin, V., Huenerbein, A., 2003. Assessing climate forcings of the Earth system for the past millennium. Geophysical Research Letters 30 (6), 1276.

Berger, A.L., 1978. Long-term variations of daily insolation and Quaternary climatic changes. Journal of Atmospheric Sciences 35, 2363–2367.

Bertrand, C., Loutre, M.F., Crucifix, M., Berger, A., 2002. Climate of the last millennium: a sensitivity study. Tellus 54A, 221–244.

Boucher, O., Pham, M., 2002. History of sulfate aerosol radiative forcings. Geophysical Research Letters 29 (9), 1308.

Bradley, R.S., 2000. 1000 years of climate change. Science 288, 1353–1354.

Bradley, R.S., Jones, P.D. (Eds.), 1992. Climate Since A.D. 1500. Routledge, London 679pp.

Bradley, R.S., Jones, P.D., 1993. 'Little Ice Age' summer temperature variations: their nature and relevance to recent global warming trends. Holocene 3, 367–376.

Bradley, R.S., Hughes, M.K., Diaz, H.F., 2003. Climate in Medieval time. Science 302, 404–405.

Briffa, K.R., 2000. Annual variability in the Holocene: interpreting the message of ancient trees. Quaternary Science Reviews 19, 87–105.

Briffa, K.R., Osborn, T.J., 2002. Blowing hot and cold. Science 295, 2227–2228.

Briffa, K.R., Jones, P.D., Bartholin, T.S., Eckstein, D., Schweingruber, F.H., Karlèn, W., Zetterberg, P., Eroren, M., 1992. Fennoscandian summers from AD 500: temperature changes on short and long timescales. Climate Dynamics 7, 111–119.

Briffa, K.R., Jones, P.D., Schweingruber, F.H., Osborn, T.J., 1998. Influence of volcanic eruptions on Northern Hemipshere summer temperature over the last 600 years. Nature 393, 450–455.

Briffa, K.R., Osborn, T.J., Schweingruber, F.H., Harris, I.C., Jones, P.D., Shiyatov, S.G., Vaganov, E.A., 2001. Low-frequency temperature variations from a northern tree ring density. Journal of Geophysical Research 106, 2929–2941.

Brovkin, V., Bendtsen, J., Claussen, M., Ganopolski, A., Kubatzki, C., Petoukhov, V., Andreev, A., 2002. Carbon cycle, vegetation and climate dynamics in the Holocene: experiments with the CLIMBER-2 model. Global Biogeochemical Cycles 16.

Campin, J.M., Goosse, H., 1999. Parameterization of density-driven downsloping flow for a coarse-resolution ocean model in z-coordinate. Tellus 51A, 412–430.

Charlson, R.J., Langner, J., Rodhe, H., Leovy, C.B., Warren, S.G., 1991. Perturbation of the Northern Hemisphere radiative balance by backscattering from anthropogenic sulfate aerosols. Tellus 43AB, 152–163.

Collins, M., Osborn, T.J., Tett, S.F.B., Briffa, K.R., Schweingruber, F.H., 2002. A comparison of the variability of a climate model with paleotemperature estimates from a network of tree-ring densities. Journal of Climate 15, 1497–1515.

Cook, E.R., D'Arrigo, R.D., Mann, M.E., 2002. A well-verified, multiproxy reconstruction of winter North Atlantic Oscillation Index since 1400 AD. Journal of Climate 15, 1754–1764.

Crowley, T.J., 2000. Causes of climate change over the past 1000 years. Science 289, 270–277.

Crowley, T.J., Lowery, T.S., 2000. How warm was the Medieval Warm Period? Ambio 29, 51–54.

Cubasch, U., Voss, R., Hegerl, G.C., Waszkewitz, J., Crowley, T.J., 1997. Simulation of the influence of solar radiation variations on the global climate with an ocean–atmosphere general circulation model. Climate Dynamics 13, 757–767.

Delworth, T.L., Manabe, S., Stouffer, R.J., 1993. Interdecadal variations of the thermohaline circulation in a coupled ocean–atmosphere model. Journal of Climate 6, 1993–2011.

Esper, J., Cook, E.R., Schweingruber, F.H., 2002. Low-frequency signals in long tree-ring chronologies for reconstructing past temperature variability. Science 295, 2250–2253.

Fichefet, T., Morales Maqueda, M.A., 1997. Sensitivity of a global sea ice model to the treatment of ice thermodynamics and dynamics. Journal of Geophysical Research 102, 12,609–12,646.

Gerber, S., Joos, F., Brugger, P., Stocker, T.F., Mann, M.E., Sitch, S., Scholze, M., 2003. Constraining temperature variations over the last millennium by comparing simulated and observed atmospheric CO_2. Climate Dynamics 20, 281–299.

Gent, P.R., McWilliams, J.C., 1990. Isopycnal mixing in ocean general circulation models. Journal Physical Oceanography 20, 150–155.

Gillett, N.P., Allen, M.R., Williams, K.D., 2002. The role of stratospheric resolution in simulating the Arctic Oscillation response to greenhouse gases. Geophysical Research Letters 29 (10).

Gillett, N.P., Zwiers, F.W., Weaver, A.J., Stott, P.A., 2003. Detection of human influence on sea-level pressure. Nature 422, 292–294.

Gonzalez-Rouco, F., von Storch, H., Zorita, E., 2003. Deep soil temperature as proxy for surface air-temperature in a coupled model simulation of the last thousand years. Geophysical Research Letters 30 (21), 2116.

Goosse, H., Fichefet, T., 1999. Importance of ice–ocean interactions for the global ocean circulation: a model study. Journal of Geophysical Research 104, 23,337–23,355.

Goosse, H., Renssen, H., 2003. Simulating the evolution of the Arctic climate during the last millennium. Seventh AMS Conference on Polar Meteorology and Oceanography, 1.5 (available at http://www.astr.ucl.ac.be/users/hgs/ams_arctic.pdf).

Goosse, H., Renssen, H., 2004. Exciting natural modes of variability by solar and volcanic forcing: idealized and realistic experiments. Climate Dynamics 23, 153–163.

Goosse, H., Renssen, H., 2005. A simulated reduction in Antarctic sea-ice area since 1750: implications of the long memory of the ocean. International Journal of Climatology (in press).

Goosse, H., Deleersnijder, E., Fichefet, T., England, M., 1999. Sensitivity of a global ocean-sea ice model to the parameterization of vertical mixing. Journal of Geophysical Research 104, 13,681–13,695.

Goosse, H., Selten, F.M., Haarsma, R.J., Opsteegh, J.D., 2001. Decadal variability in high northern latitudes as simulated by an intermediate complexity climate model. Annals of Glaciology 33, 525–532.

Goosse, H., Masson-Delmotte, V., Renssen, H., Delmotte, M., Fichefet, T., Morgan, V., van Ommen, T., Khim, B.K., Stenni, B., 2004. A late medieval warm period in the Southern Ocean as delayed response to external forcing? Geophysical Research Letters 31 (6), L06203.

Griffies, S.M., Bryan, K., 1997. A predictability study of simulated North Atlantic multidecadal variability. Climate Dynamics 13, 459–487.

Grötzner, A., Latif, M., Timmermann, A., Voss, R., 1999. Interannual to decadal climate predictability in a coupled ocean–atmosphere General Circulation Model. Journal of Climate 12, 2607–2624.

Grove, J.M., 2001. The initiation of the "Little Ice Age" in regions around the North Atlantic. Climatic Change 48, 53–82.

Hegerl, G.C., North, G.R., 1997. Comparison of statistically optimal approaches to detecting anthropogenic climate change. Journal of Climate 10, 1125–1133.

Hughes, M.K., Diaz, H.F., 1994. Was there a "Medieval Warm Period", and if so, where and when? Climatic Change 26, 109–142.

Jones, P.D., Briffa, K.R., Barnett, T.P., Tett, S.F.B., 1998. High-resolution palaeoclimatic records for the last millennium: interpretation, integration and comparison with General Circulation Model control-run temperatures. The Holocene 8, 455–471.

Jones, P.D., Osborn, T.J., Briffa, K.R., 2001. The evolution of climate over the last millennium. Science 292, 662–666.

Jones, P.D., Briffa, K.R., Osborn, T.J., 2003. Changes in the Northern Hemisphere annual cycle: implications for paleoclimatology. Journal of Geophysical Research 108, 4588.

Lean, J., Beer, J., Bradley, R., 1995. Reconstruction of solar irradiance since 1610: implications for climate change. Geophysical Research Letters 22, 1591–1594.

Lorenz, E.N., 1975. Climate predictability. In: The Physical Bases of Climate and Climate modeling, GARP Publication Series, vol. 6. World Meteorological Organisation, pp. 132–136.

Luterbacher, J., Xoplaki, E., Dietrich, D., Jones, P.D., Davies, T.D., Portis, D., Gonzalez-Rouco, J.F., von Storch, H., Gyalistras, D., Casty, C., Wanner, H., 2002. Extending North Atlantic Oscillation reconstructions back to 1500. Atmospheric Science Letters 2, 114–124.

Luterbacher, J., Dietrich, D., Xoplaki, E., Grosjean, M., Wanner, H., 2004. European seasonal and annual temperature variability, trends, and extremes since 1500. Science 303 (5663), 1499–1503.

Mann, M.E., Bradley, R.S., Hughes, M.K., 1999. Northern Hemisphere temperatures during the past millennium: inferences, uncertainties, and limitations. Geophysical Research Letters 26, 759–762.

Mann, M.E., Gille, E., Bradley, R.S., Hughes, M.K., Overpeck, J., Keimig, F.T., Gross, W., 2000. Global temperature patterns in past centuries: an interactive presentation. Earth Interactions 4, 4.

Manabe, S., Spelman, M.J., Stouffer, R.J., 1992. Transient responses of a coupled atmosphere-ocean model to gradual changes of atmospheric CO_2. II. Seasonal response. Journal of Climate 4, 105–126.

Meehl, G.A., Washington, W.M., Wigley, T.M., Arblaster, J.M., Dai, A., 2002. Solar and greenhouse gas forcing and climate response in the twentieth century. Journal of Climate 16, 426–444.

Mellor, G.L., Yamada, T., 1982. Development of a turbulence closure model for geophysical fluid problems. Reviews of Geophysics and Space Physics 20, 851–875.

Opsteegh, J.D., Haarsma, R.J., Selten, F.M., Kattenberg, A., 1998. ECBILT: a dynamic alternative to mixed boundary conditions in ocean models. Tellus 50A, 348–367.

Overpeck, J., Hughen, K., Hardy, D., Bradley, R., Case, R., Douglas, M., Finney, B., Gajewski, K., Jacoby, G., Jennings, A., Lamoureux, S., Lasca, A., MacDonald, G., Moore, J., Retelle, M., Smith, S., Wolfe, A., Zielinski, G., 1997. Arctic environmental change of the last four centuries. Science 278, 1251–1256.

Paeth, H., Latif, M., Hense, A., 2003. Global SST influence on twentieth century NAO variability. Climate Dynamics 21, 63–75.

Ramankutty, N., Foley, J.A., 1999. Estimating historical changes in global land cover: croplands from 1700 to 1992. Global Biogeochemical Cycles 13, 4:997–1027.

Renssen, H., Goosse, H., Fichefet, T., 2002. Modeling the effect of freshwater pulses on the early Holocene climate: the influence of high-frequency climate variability. Paleoceanography 17, 1020.

Rind, D., Lean, J., Healy, R., 1999. Simulated time-dependent response to solar radiative forcing since 1600. Journal of Geophysical Research 104, 1973–1990.

Robertson, A., Overpeck, J., Rind, D., Mosley-Thompson, E., Zielinski, G., Lean, J., Koch, D., Penner, J., Tegen, I., Healy, R., 2001. Hypothesized climate forcing time series for the last 500 years. Journal of Geophysical Research 106, 14783–14803.

Rossow, W.B., Walker, A.W., Beuschel, D.E., Roiter, M.D., 1996. International satellite cloud climatology project (ISCCP) documentation of new cloud datasets. WMO/TD-No 737. World Meteorological Organisation.

Selten, F.M., Haarsma, R.J., Opsteegh, J.D., 1999. On the mechanism of North Atlantic decadal variability. Journal of Climate 12, 1956–1973.

Shabalova, M.V., Van Engelen, F.V., 2003. Evaluation of a reconstruction of winter and summer temperatures in the low countries, AD 764-1998. Climatic Change 58, 219–242.

Shindell, D.T., Miller, R.L., Schmidt, G.A., Pandolfo, L., 1999. Simulation of recent northern winter climate trends by greenhouse-gas forcing. Nature 399, 452–456.

Shindell, D., Schmidt, G.A., Mann, M.E., Rind, D., Waple, A., 2001. Solar forcing of regional climate change during the Maunder Minimum. Science 294, 2149–2152.

Stott, P.A., Tett, S.F.B., 1998. Scale-dependent detection of climate change. Journal of Climate 11, 3282–3294.

Stott, P.A., Tett, S.F.B., Jones, G.S., Allen, M.R., Mitchell, J.F.B., Jenkins, G.J., 2000. External control of 20th century temperature by natural and anthropogenic forcing. Science 290, 2133–2137.

Thomson, D.J., 1995. The seasons, global temperature, and precession. Science 268, 59–68.

Timmermann, A., Latif, M., Voss, R., Grötzner, A., 1998. Northern Hemispheric Interdecadal Variability: a coupled Air–Sea Mode. Journal of Climate 11, 1906–1931.

van der Schrier, G., Weber, S.L., Drijfhout, S.S., 2002. Sea level changes in the North Atlantic by solar forcing and internal variability. Climate Dynamics 19, 435–447.

Villalba, R., 1990. Climatic fluctuations on Northern Patagonia during the last 1000 years as inferred from tree-ring records. Quaternary Research 34, 346–360.

Waple, A.M., Mann, M.E., Bradley, R.S., 2002. Long-term patterns of solar irradiance forcing in model experiments and proxy based surface temperature reconstructions. Climate Dynamics 18, 563–578.

Widmann, M., Tett, S.F.B., 2003. Simulating the climate of the last millennium. Pages News 11, 21–23.

Wilks, D.S., 1995. Statistical Methods in the Atmospheric Sciences. Academic Press, San Diego 467pp.

Zorita, E., González-Rouco, F., 2000. Disagreement between predictions of the future behavior of the Arctic Oscillation as simulated in two different climate models: implications for global warming. Geophysical Research Letters 27, 1755–1758.